Journal of Medicinal Chemistry

Brief Article

pubs.acs.org/jmc

# Efficient Palladium-Triggered Release of Vorinostat from a Bioorthogonal Precursor

Belén Rubio-Ruiz,[†] Jason T. Weiss,[†,‡] and Asier Unciti-Broceta*[,†]

[†]Cancer Research UK Edinburgh Centre, Institute of Genetics and Molecular Medicine, University of Edinburgh, Crewe Road South, Edinburgh EH4 2XR, U.K.

Supporting Information

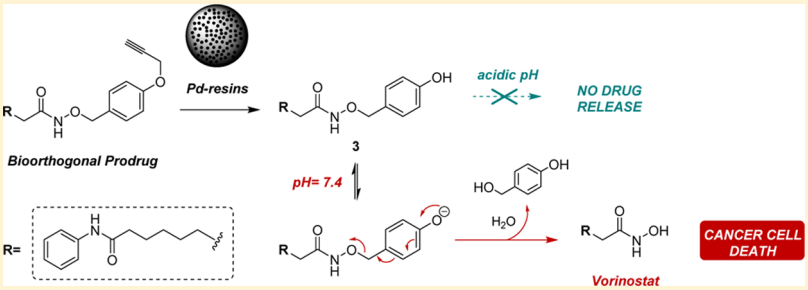


**ABSTRACT:** Bioorthogonal uncaging strategies have recently emerged as an experimental therapeutic approach to control drug release. Herein we report a novel masking strategy that enables to modulate the metal chelating properties of hydroxamic acid groups by bioorthogonal chemistry using Pd-functionalized resins. This novel approach allowed to devise an inactive precursor of the histone deacetylase inhibitor vorinostat that was efficiently uncaged by heterogeneous Pd catalysis in cell culture models of glioma and lung cancer.

## INTRODUCTION

The activation of prodrugs by benign chemical processes that are not reliant on intrinsic biological mediators have the potential to achieve a superior control over the area where drugs are generated (e.g., tissues, organs, cells), thus minimizing untoward drug release and consequent adverse effects. The feasibility of such an approach has been recently demonstrated in cancer cell culture with two different strategies: metal-free click-to-release chemistry[1−3] and transition metal-mediated bioorthogonal deprotection chemistry.[4−8] The latter strategy provides a nonenzymatic method to trigger multiple drug-uncaging cycles per catalyst molecule. It has also been shown that in vivo surgical insertion of Pd-functionalized implants (= extracellular heterogeneous catalysts) can be used to mediate local uncaging of systemically administered drug surrogates in zebra fish.[4,5] As a molecularly targeted version of this strategy, the use of Ru- and Pd-loaded nanodevices with cell targeting capabilities has been proposed to track single cancer cells and individually treat them following administration of transition metal-activated drug precursors.[8−11]

One of the distinctive opportunities offered by the application of bioorthogonal activation methods in cancer therapy is that it could be exploited to uncage multiple specifically designed chemotherapy precursors using the same triggering stimulus, thus enabling the controlled release, concurrent or successively, of synergistic therapeutics at the same anatomical area (e.g., inside a tumor where a Pd-functionalized device has been inserted). Such an approach may offer a safer way to treat locally advanced cancers through drug combinations and, potentially, overcome chemoresistance. Encouraged by this, our lab is exploring new chemistries to develop novel caged chemotherapeutic agents that are specifically released by bioorthogonal means, particularly via heterogeneous Pd catalysis.[4−7] To design an efficient bioorthogonal prodrug, it is fundamental to identify and mask the drug's functional group that is most essential for its cytotoxic mode of action. Importantly, the designated masking group has to be resistant to metabolic processing and cleavable by the triggering mechanism of choice at physiological conditions (water, 37 °C, pH ∼ 7, isotonicity). Although several bioorthogonal uncaging reactions have been reported in recent years,[12] they all can be grouped in two classes: the deprotection of carbamate-masked primary amino groups[1−5,13−15] and the *N*-depropargylation of endocyclic nitrogen atoms with lactam−lactim tautomerism.[4,6,7] As the cytotoxicity of many therapeutic agents is modulated by other chemical functionalities, there is a need for an expanded set of bioorthogonal masking strategies that could be accommodated to such functional groups and thus increase the diversity of bioorthogonally activated prodrugs. This is, for example, the case of hydroxamic acid-based drugs, which are currently used in the clinic for the treatment of different disorders including iron-overload disease,[16] cancer,[17] and infections,[18] and whose pharmacological activity is endowed by the metal-chelating capacity of their hydroxamic acid group.

**Received:** September 28, 2016
**Published:** October 27, 2016





DOI: 10.1021/acs.jmedchem.6b01426
*J. Med. Chem.* XXXX, XXX, XXX−XXX

**Scheme 1. (a) Binding Interactions between 1 and HDAC8 and (b) Proposed Masking Strategy**[a]

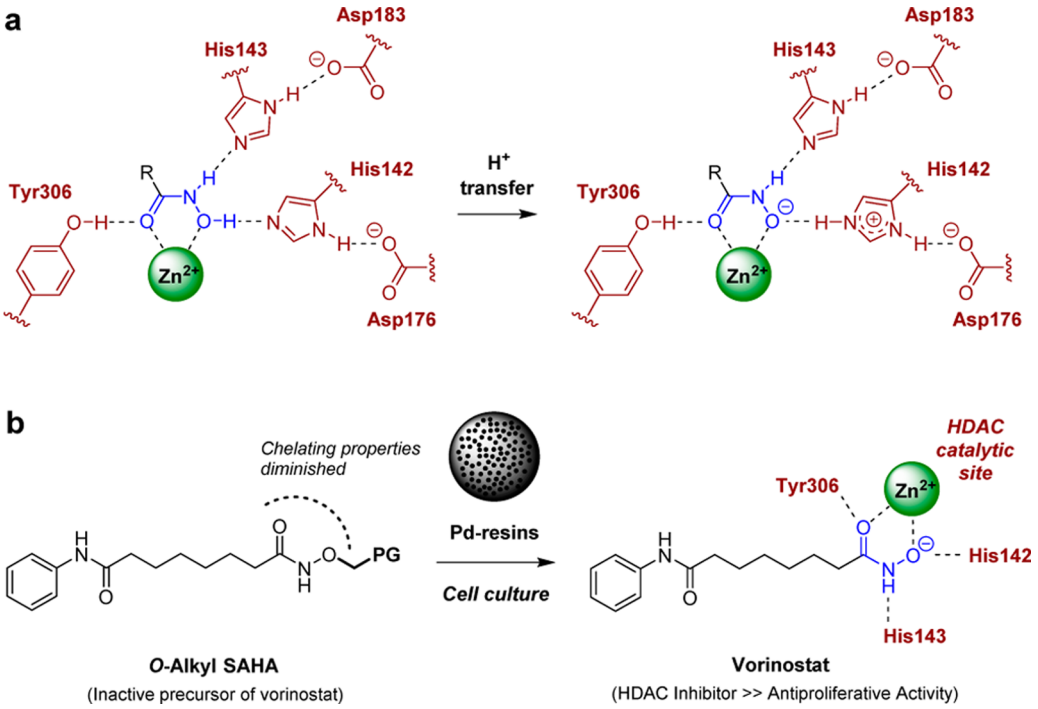


[a]Upon coordination, the p$K_a$ of the hydroxamic acid group drops and the OH proton transferred to the imidazole group of His142. The generated anion further strengthens the coordinative bond between the drug and the $Zn^{2+}$ atom of the enzyme.[25]

**Scheme 2. (a) Synthesis of *O*-Alkyl SAHA Derivatives 2a–e and (b) $FeCl_3$ Colorimetric Test**[a]

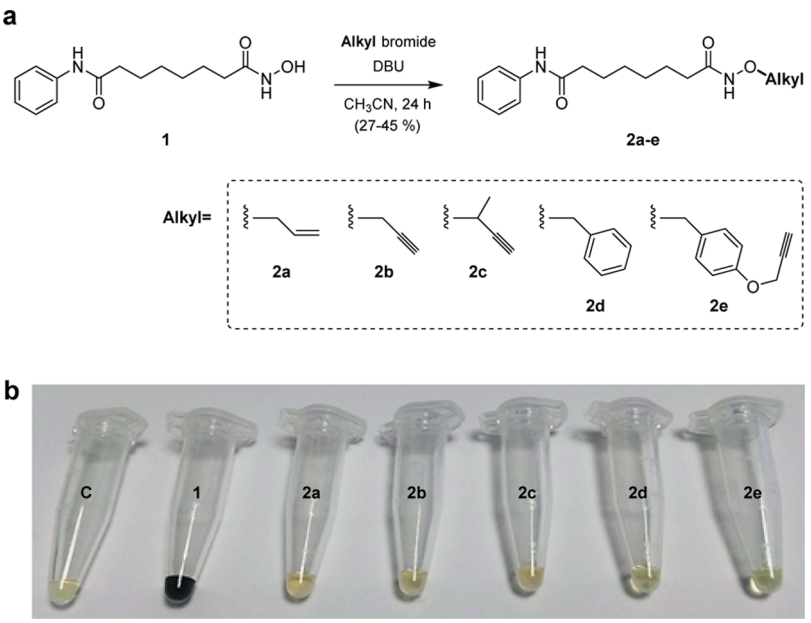


[a]**1** and **2a–e** were independently dissolved in a water–ethanol mixture (concentration = 40 mM). Each solution was subsequently mixed with an equal volume of $FeCl_3$ (80 mM in water–ethanol) and imaged. C = DMSO + $FeCl_3$.

## RESULTS AND DISCUSSION

**Rationale for Prodrug Design.** Histone deacetylases (HDACs) belong to a class of enzymes that catalyzes the removal of acetyl groups from $^{\varepsilon}$*N*-acetylated lysine residues of DNA-binding proteins called histones, resulting in a tight chromatin structure where gene expression is significantly repressed.[19−22] The antitumor activity of HDAC inhibitors is mainly a consequence of transcriptional changes in genes involved in oncogenesis.[19] The characteristic presence of multiple expression defects in transformed cells[20] and their sensitivity to oxidative damage[21] have been proposed as the essential features for the preferential activity of HDAC inhibitors over cancer cells. Nevertheless, these inhibitors suffer from dose-limiting side effects due to the central role of HDACs in normal cells.[22]


DOI: 10.1021/acs.jmedchem.6b01426
J. Med. Chem. XXXX, XXX, XXX−XXX

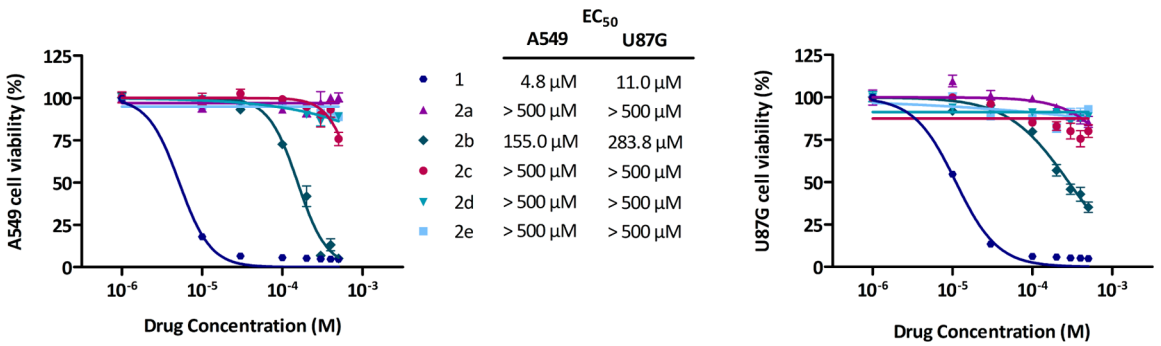


**Figure 1.** Half-log dose response curves and calculated $EC_{50}$ values of **1** and **2a**–**e** after 5 d incubation with NSCLC A549 cells and glioma U87G cells.

**Scheme 3. Pd-Triggered Uncaging of Compound 2e**[a]

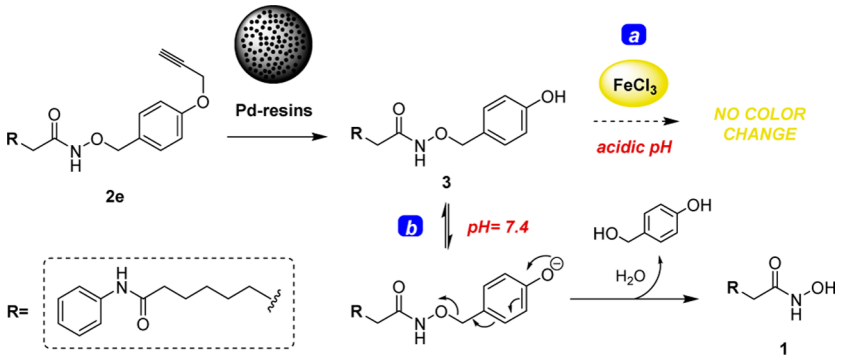


[a]Conditions: (a) Treatment of **2e** (4 mM) with Pd resins (10 mg/mL) and $FeCl_3$ (8 mM) in a water/ethanol solution for 24 h resulted in no color change under these conditions. LCMS proved formation of intermediate **3**. (b) Treatment of **2e** (0.1 mM) with Pd resins (1 mg/mL) in PBS at 37 °C for 24 h resulted in the formation of **1**.

Suberoylanilide hydroxamic acid (SAHA), **1**, aka vorinostat, was the first HDAC inhibitor to be approved by the FDA to treat cancer.[21−25] It is currently indicated for the treatment of cutaneous T cell lymphoma and under clinical investigation for recurrent glioblastoma multiforme and advanced nonsmall-cell lung carcinoma (NSCLC). X-ray analysis[24] determined that the main binding interactions between vorinostat and its target are mediated through the hydroxamic acid group, which doubly coordinates to a zinc atom at the catalytic site of the enzyme (Scheme 1a).[25]

On the basis of this mode of binding, alkylation of the OH group of the hydroxamic acid (Scheme 1b) is expected to result in a significant reduction of its chelating properties and, consequently, of the capacity of **1** to inhibit its target(s). In addition, we envisaged that, as opposed to carboxylic esters and amides, *O*-alkyl hydroxamates would be resistant to enzymatic hydrolysis, as neither esterases nor amidopeptidases should recognize this functional group. Consequently, this straightforward derivatization of bioactive hydroxamic acids could in principle facilitate the generation of derivatives that are both pharmacologically inactive and metabolically stable, two essential features for the successful generation of bioorthogonal prodrugs.

**Synthesis of Pd-Activated Prodrugs 2a−e.** We and others have shown that propargyl groups attached to functionalities bearing moderately acidic hydrogen atoms ($pK_a \sim 9$), such as aromatic $\delta$-lactams[4,6,7] and phenolic alcohols,[26,27] are readily cleaved by Pd species in biocompatible environs. Because the reported $pK_a$ of aliphatic hydroxamic acid groups is 9.4,[25] a selection of *O*-alkylated hydroxamates of **1** was prepared by direct treatment of **1** with the corresponding alkyl bromides, including propargyl and 4-(propargyloxy)benzyl bromides, and DBU (Scheme 2a).

**Study of the Iron Chelating Capacity of Compounds 1 and 2a−e.** A remarkable feature of hydroxamic acids is their ability to form strongly colored coordination complexes with ferric ions.[16] Such a capacity should be either lost or greatly diminished in compounds **2a**−**e**. As the chelating properties of **1** are essential for its bioactivity, this reaction was used as a colorimetric test to measure the efficacy of the masking strategy. As expected, treatment of **1** with a solution of $FeCl_3$ (water/ethanol solution) produced a dark-violet mixture (Scheme 2b), proving its potent affinity for ferric cations (siderochrome). On the contrary, **2a**−**e** did not induce any color change relative to the negative control (DMSO + $FeCl_3$), even at high concentrations (20 mM), thus indicating that the chelating properties of these derivatives are abolished by the alkyl promoiety attached to the hydroxamic OH group. Because of the striking differences between the coordination properties of **1** and **2a**−**e**, we conveniently used a $FeCl_3$ solution as a TLC staining reagent during synthesis.

**Bioorthogonality Study.** Along with rendering the drug precursor responsive to a specific triggering stimulus, an optimal prodrug design should be capable of reducing a drug's bioactivity at significant levels, preferably 2 orders of magnitude.[4] To determine the bioorthogonality[5] of the *O*-alkyl hydroxamates in cancer cells, dose response studies were performed for **1** and **2a**−**e** in NSCLC A549 cells and glioma U87G cells. As shown in Figure 1, *O*-alkyl SAHA derivatives **2a**−**e** mediated patently lower cytotoxicity than the parent drug


DOI: 10.1021/acs.jmedchem.6b01426
J. Med. Chem. XXXX, XXX, XXX−XXX

**1** in both cell lines, highlighting the low activity observed for derivative **2e**, with a projected $EC_{50}$ (**2e**)/$EC_{50}$ (**1**) value far beyond 2 orders of magnitude. Interestingly, the difference in activity between the *O*-propargyl derivative **2b** and **1** was more modest ($EC_{50}$ (**2b**)/$EC_{50}$ (**1**) = 20−30), which might be due to limited intracellular stability. To the best of our knowledge, this study is the first to show a qualitative correlation between the metal chelating properties of the hydroxamic acid group and the antiproliferative activity of the corresponding derivative and further corroborates the role played by such a functional group in the bioactivity of **1**.

**Prodrug Activation Studies: In Vitro and in Cell Culture.** The Pd-mediated release of **1** from nonchelating *O*-alkyl SAHA derivatives **2a**−**e** was tested next. $FeCl_3$ was mixed with each derivative and treated with a heterogeneous Pd catalyst (Pd-resins containing 4.62% w/w in $Pd^0$ nanoparticles captured in a PEG-grafted polystyrene matrix of 150 $\mu$m in diameter[4]). As shown in Supporting Information (SI), Figure S1, no color change (= no release of **1**) was observed after incubating the benzyl derivative **2d** with Pd resins for 24 h. In contrast, the solution of the propargyl and 1-butyn-3-yl derivatives **2b**,**c** turned to violet just after 3 h and the color intensity increased with time, suggesting formation of **1**, while the allyl derivative **2a** showed much lower sensitivity to Pd resins. Treatment of **2e** and Pd resins did not result in color variation, although discoloration of the mixture suggested that a reaction did occur. Rather than due to the inability of Pd to cleave the *O*-propargyl group, we presumed that the lack of color change was due to the inhibited elimination of the self-immolative linker of the depropargylated intermediate **3** under the reaction conditions (Scheme 3, conditions a), a process that is expected to be influenced by the pH.[28] This was confirmed by LCMS (SI, Figure S2).

We then investigated the deprotection of derivatives **2b**,**c** and **2e** in the presence of Pd resins under physiological conditions, i.e., 37 °C in PBS (pH = 7.2−7.4). Reactions were monitored for 24 h by HPLC (UV detector). In agreement with the colorimetric tests, **2b**,**c** rapidly reacted with Pd resins under these conditions. However, the reactions did not only result in the generation of **1**. The disappearance of **2b**,**c** and the formation of two uncharacterized products were observed just after 3 h, with **1** being a minor product of the reaction (see SI, Figures S3,S4). Remarkably, reaction of **2e** with Pd resins under such conditions (Scheme 3, conditions b) resulted in the quantitative generation of **1** (SI, Figure S5). As shown in SI, Figure S6, most of **2e** was cleaved after 3 h and two new species appeared in the chromatogram: *O*-(4-hydroxybenzyl) SAHA, **3**, and **1** (identified by LCMS, SI, Figure S5). After 6 h incubation, the major product was **1**, showing that the self-immolative linker of **3** is labile at physiological pH. This is noteworthy because it represents the first successful use of a self-immolative linker capable of undergoing a 1,6-benzyl elimination as a masking strategy for hydroxamic acids. In fact, previous work from Cohen and co-workers reported that *O*-hydroxybenzyl benzohydroxamate (an aromatic hydroxamic acid) is stable in water (HEPES buffer, pH = 7.5),[29] which may have discouraged further investigations in this direction.

The disappearance in absorbance of **2e** at 254 nm at different time points was used to make a kinetics plot (SI, Figure S7) and to calculate the rate constant of the *O*-depropargylation reaction in physiological conditions: $3.8 \times 10^{-4}$ $M^{-1}$ $s^{-1}$ ($t_{1/2}$ = 30 min), which is slightly slower than classical homogeneous CuAAC reactions[30] but much faster than previous heterogeneous Pd-mediated prodrug activations.[4,6,7] Reaction of **2e** with Pd resins in mildly acidic media (pH = 6.0) resulted in the deceleration, *but not inhibition*, of the pH-dependent 1,6-elimination step (SI, Figures S8,S9). Interestingly, the acidic environment showed no effect over the kinetics of the *O*-depropargylation reaction. Because the 4-hydroxybenzyl motif can be found in natural compounds such as the amino acid tyrosine, a residue that is involved in the regulation of many biochemical processes including ligand−receptor recognition events or auto/trans-phosphorylation reactions, the scope of the *O*-propargylation method herein described should be extendable to additional applications of interest in medicinal chemistry and chemical biology such as the bioorthogonal regulation[14] of peptides and proteins' bioactivity (e.g., kinase activity) by Pd chemistry in physiological environments.

Next, the Pd-triggered release of **1** from **2a**−**e** was investigated in cancer cell culture using A549 and U87G cells as cancer cell models. Cells were treated with Pd resins (1 mg/mL) and **2a**−**e** (100 $\mu$M) separately (negative controls) or in combination (activation assay) and unmodified **1** (100 $\mu$M) used as the positive control.

As shown in Figure 2, **2a**,**d** showed low or null bioactivity regarless of the presence and absence of Pd resins. Interestingly,

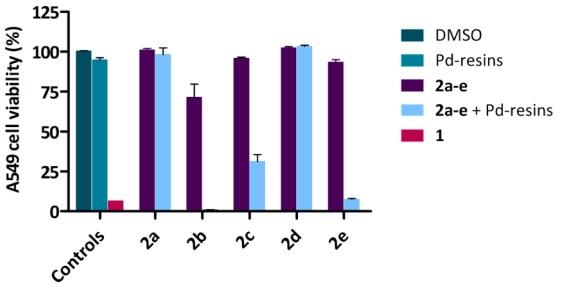


**Figure 2.** Antiproliferative activity of **2a**−**e** in A549 cells after incubation with or without Pd resins for 5 d. Controls: untreated cells (dark green), cells treated with Pd resins (light green) or **1** (red).

**2b** and **2c** reduced the viability of cancer cells in combination with the Pd source, indicating that the unknown products formed in the process might also possess bioactivity. As expected (see Figure 2), **2e** elicited a potent cytotoxic effect only in the presence of the heterogeneous catalyst (= implantable device). The observed antiproliferative effect was equivalent to that mediated by **1**, suggesting that the active drug is rapidly released in standard cell culture conditions. These results were further corroborated by time lapse imaging using an IncuCyte ZOOM device. As shown in Figure 3a,b, cells incubated with either **2e** or Pd resins showed a growth curve equal to that of untreated cells (DMSO), whereas the **2e**/Pd resins combination (in blue) displayed a cytotoxic effect identical to that of cells incubated with the parental drug (in red).

Dose response study of **2e** alone or in combination with Pd resins demonstrated concentration dependent cytotoxic effect in the presence of the catalyst, with complete innocuity in its absence (Figure 3c and SI, Figure S10).

**Target Engagement Study.** In situ formation of **1** was verified by studying intracellular target displacement of the fluorescent HDAC inhibitor coumarin−SAHA, **4** (Figure 4a). As reported by Srivastava et al.,[31] the blue-emitting fluorescent properties of this closely related analogue of **1** are quenched in cells after binding to HDACs. Competitive displacement from


DOI: 10.1021/acs.jmedchem.6b01426
J. Med. Chem. XXXX, XXX, XXX−XXX

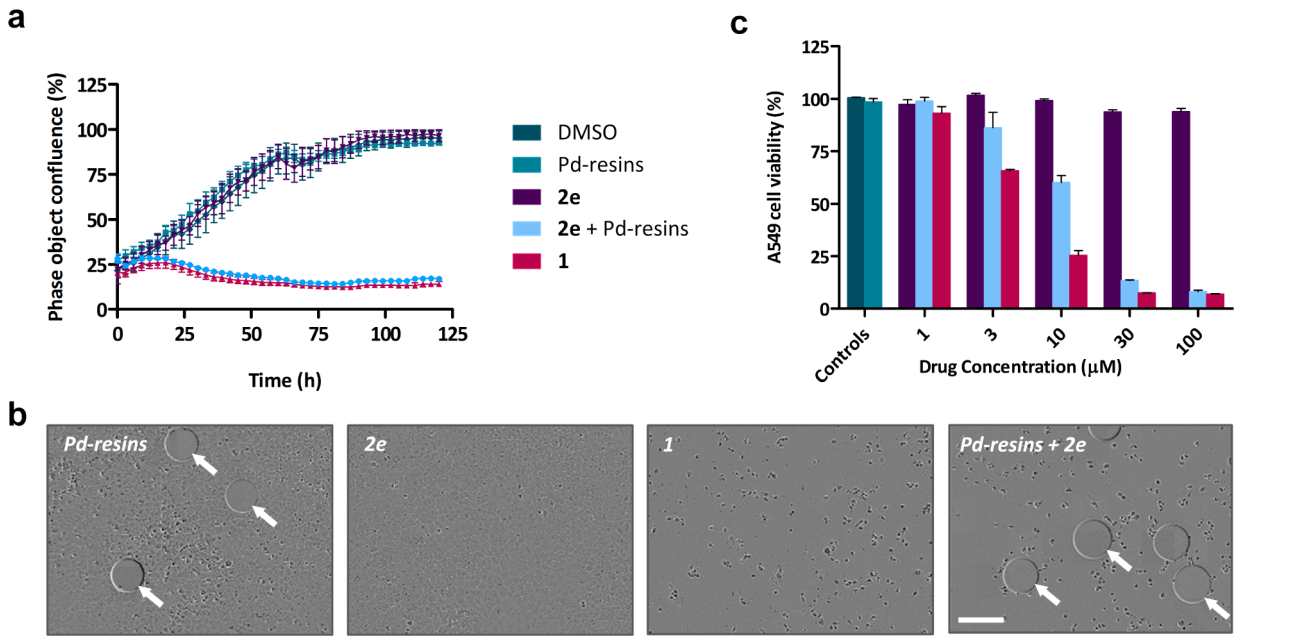


**Figure 3.** (a) Real-time growth curves of A549 cells under treatment for 5 d. Drug (**1**)/prodrug (**2e**) concentrations: 100 $\mu$M. Cell growth was monitored using an IncuCyte system in an incubator (5% $CO_2$, 37 °C). Error bars: ± SD from $n$ = 3. (b) Images of A549 cells after 5 d treatment with (from left to right) 1 mg/mL of Pd resins, 100 $\mu$M of **2e**, 100 $\mu$M of **1**, or combination of both. Pd resins are identified with arrows. Scale bar: 300 $\mu$m. (c) Half-log dose response study (1−100 $\mu$M) of **2e** cytotoxic activity in the presence and absence of Pd resins in A549 cells. Controls: untreated cells (dark green), cells treated with Pd-resins (light green), or **1** (red). Cell viability was measured at day 5 using PrestoBlue reagent. Error bars: ± SD from $n$ = 3.

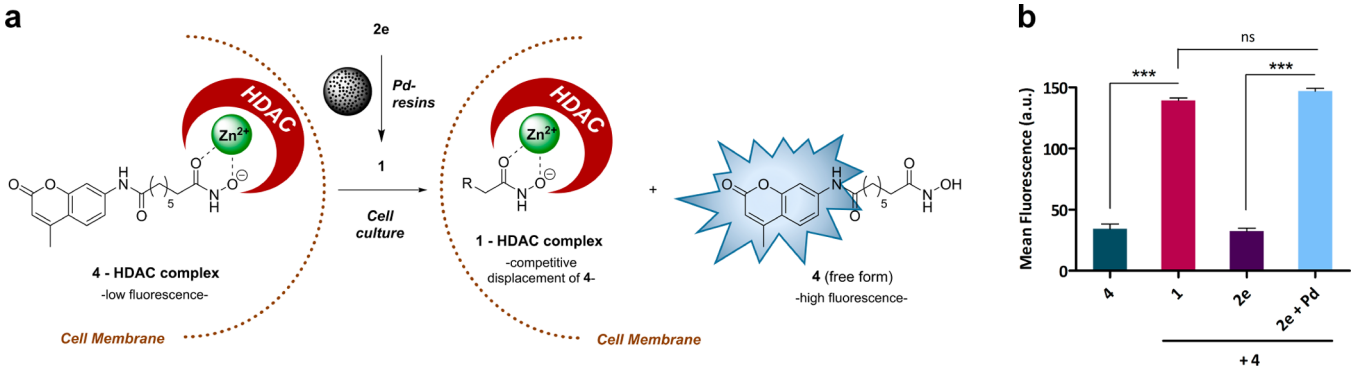


**Figure 4.** (a) Fluorescent assay designed to prove the in situ synthesis of **1** from **2e** via Pd chemistry. Upon release of **1**, quenched compound **4** is competitively displaced from the catalytic site of the enzyme, resulting in a fluorescent signal ($\lambda_{ex/em}$ = 405/450 nm). (b) Mean fluorescence of A549 cells analyzed by flow cytometry after treatment with **4** (6 h) followed by addition of either DMSO, **1**, **2e**, or **2e**/Pd resin combinations (12 h). Error bars: ± SD from $n$ = 3; $p$ < 0.001, *** (ANOVA).

the target's binding site restores its fluorescent properties and thus can be used to study specific target engagement. A549 cells were incubated with **4** (10 $\mu$M) for 6 h, followed by addition (100 $\mu$M) of either **1**, **2e**, or **2e**/Pd resins combination and incubation for 12 h. Cell fluorescence intensity was studied by flow cytometry ($\lambda_{ex/em}$ = 405/450 nm). As shown in Figure 4b, cotreatment of **4** with nonchelating precursor **2e** did not induce any change in fluorescence emission, thus demonstrating that this derivative does not interact with HDACs and is biochemically stable. In contrast, cells pretreated with **4** and incubated with **2e** in the presence of Pd resulted in a highly significant increase of fluorescence signal, which was equivalent to the increment observed by direct cotreatment with unmodified compound **1**.

## CONCLUSIONS

HDAC inhibitors are a distinct class of pharmaceuticals that target the abnormal epigenetic states found in different disorders, including cancer. **1** was the first HDAC inhibitor to reach the clinic for the treatment of cutaneous T cell lymphoma, and it has shown great promise in other malignancies.[21−25] However, both its systemic side effects (e.g., hematological problems, cardiotoxicity, etc.) and its poor pharmacokinetics properties ($t_{1/2}$ in human serum is 1.5 h)[32] have limited its clinical use. Consequently, a number of research groups have attempted to circumvent the liabilities of **1** by developing prodrugs designed to be activated through a range of biochemical processes.[32−34]

Herein we have reported a novel strategy that enabled, for the first time, to devise a completely inactive precursor of **1** that is rapidly uncaged by a bioorthogonal activation method in cell


DOI: 10.1021/acs.jmedchem.6b01426
J. Med. Chem. XXXX, XXX, XXX−XXX

models of cancer. The deprotection proceeds via a tandem mechanism triggered by the Pd-catalyzed depropargylation of a phenolic ether group and followed by 1,6-elimination of a 4-hydroxybenzyl group directly attached to the OH of the drug's hydroxamic acid group, a previously unreported process that takes place at physiological pH. While important challenges remain to be solved before translating this experimental approach to the clinic (e.g., quantity of Pd required to achieve bioactive drug concentrations, long-term stability of the catalyst in vivo, use of extra vs intracellular Pd devices, etc.), extending the scope of functional groups amenable to activation by Pd chemistry will provide future therapeutic alternatives upon which to capitalize once such issues are overcome. Additionally, because of the versatility of the linker,[35] the scope of this strategy extends beyond Pd and affords manifold opportunities to modulate the chelating/bioactive properties of hydroxamic acids through bioorthogonal and biochemical stimuli.

## EXPERIMENTAL SECTION

**General.** Chemicals were purchased from Fisher Scientific, Sigma-Aldrich, or VWR. **1** and **3** were purchased from Cayman Chemical Company. NMR spectra were recorded at rt on a 500 MHz Bruker Avance III spectrometer. Chemical shifts are reported in ppm relative to the solvent peak. High resolution mass spectrometry was measured in a Bruker MicrOTOF II. Analytical TLC was performed using Merck TLC Silica Gel 60 F254 plates and visualized by UV light. Purifications were carried out by flash column chromatography using commercially available silica gel (220−440 mesh, Sigma-Aldrich). All compounds used in the biological experiments were >95% pure, as measured by HPLC using an UV−vis 254 nm detector. Method: eluent A, water and trifluoroacetic acid (0.4%); eluent B, acetonitrile, A/B = 95:5 to 20:80 in 6 min, isocratic 1 min, 20:80 to 95:5 in 0.1 min, and isocratic 2 min. Stock solutions (100 mM) were prepared in DMSO.

**Synthesis of 4-(Propargyloxy)benzyl Bromide.** 4-Hydroxylbenzyl alcohol was treated with propargyl bromide and $K_2CO_3$ to give rise 4-(propargyloxy)benzyl alcohol, which was then converted in the corresponding halogenated intermediate using $CBr_4/PPh_3$ (67%, 2 steps).[36]

**General Method for the Synthesis of 2a−e.** Vorinostat, **1** (60 mg, 0.23 mmol) and 1,8-diazabicyclo[5.4.0]undec-7-ene (0.27 mmol) were dissolved in dry acetonitrile (1 mL) under $N_2$ atmosphere and cooled to 4 °C. Either allyl bromide, propargyl bromide, 3-bromo-1-butyne, benzyl bromide, or 4-(propargyloxy)benzyl bromide (0.23 mmol) were dissolved in dry acetonitrile (0.5 mL). The solution was added dropwise to the mixture and the resulting mixture stirred at room temperature for 24 h. Solvent was then removed under reduced pressure and the crude purified via flash chromatography eluting with ethyl acetate/hexane (2:1).

*O-Allyl Suberoylanilide Hydroxamate (**2a**).* White solid (28 mg, 41% yield). $^1$H NMR (500 MHz, DMSO) $\delta$ 10.85 (s, 1H), 9.82 (s, 1H), 7.58 (d, $J$ = 7.6 Hz, 2H), 7.27 (m, 2H), 7.01 (t, $J$ = 7.4 Hz, 1H), 5.90 (ddt, $J$ = 16.6, 10.5, 6.0 Hz, 1H), 5.26 (m, 2H), 4.25 (d, $J$ = 6.0 Hz, 2H), 2.28 (t, $J$ = 7.4 Hz, 2H), 1.93 (t, $J$ = 7.3 Hz, 2H), 1.57 (m, 2H), 1.48 (m, 2H), 1.27 (m, 4H). $^{13}$C NMR (126 MHz, DMSO) $\delta$ 171.2, 169.2, 139.3, 133.2 (CH), 128.6 (2 × CH), 122.9 (CH), 119.0 (2 × CH), 118.9 ($CH_2$), 75.8 ($CH_2$), 36.3 ($CH_2$), 32.2 ($CH_2$), 28.4 ($CH_2$), 28.3 ($CH_2$), 25.0 ($CH_2$), 24.8 ($CH_2$). HRMS (ESI) $m/z$ [M + H]$^+$ calcd for $C_{17}H_{25}O_3N_2$, 305.1859; found, 305.1856.

*O-Propargyl Suberoylanilide Hydroxamate (**2b**).* White solid (27 mg, 40% yield). $^1$H NMR (500 MHz, DMSO) $\delta$ 11.09 (s, 1H), 9.82 (s, 1H), 7.58 (d, $J$ = 7.6 Hz, 2H), 7.27 (m, 2H), 7.01 (t, $J$ = 7.4 Hz, 1H), 4.43 (d, $J$ = 2.4 Hz, 2H), 3.55 (t, $J$ = 2.4 Hz, 1H), 2.28 (t, $J$ = 7.5 Hz, 2H), 1.96 (t, $J$ = 7.3 Hz, 2H), 1.57 (m, 2H), 1.49 (m, 2H), 1.28 (m, 4H). $^{13}$C NMR (126 MHz, DMSO) $\delta$ 171.2, 169.5, 139.3, 128.6 (2 × CH), 122.9 (CH), 119.0 (2 × CH), 78.9, 78.4 (CH), 62.3 ($CH_2$), 36.3 ($CH_2$), 32.1 ($CH_2$), 28.4 ($CH_2$), 28.3 ($CH_2$), 25.0 ($CH_2$), 24.7 ($CH_2$). HRMS (ESI) $m/z$ [M + H]$^+$ calcd for $C_{17}H_{23}O_3N_2$, 303.1703; found, 303.1693.

*O-1-Butyn-3-yl Suberoylanilide Hydroxamate (**2c**).* White solid (32 mg, 45% yield). $^1$H NMR (500 MHz, DMSO) $\delta$ 10.97 (s, 1H), 9.82 (s, 1H), 7.58 (d, $J$ = 7.6 Hz, 2H), 7.27 (m, 2H), 7.01 (t, $J$ = 7.4 Hz, 1H), 4.61 (q, $J$ = 6.5 Hz, 1H), 3.51 (d, $J$ = 1.6 Hz, 1H), 2.28 (t, $J$ = 7.5 Hz, 2H), 1.98 (t, $J$ = 7.3 Hz, 2H), 1.57 (m, 2H), 1.49 (m, 2H), 1.34 (d, $J$ = 6.7 Hz, 3H), 1.27 (m, 4H). $^{13}$C NMR (126 MHz, DMSO) $\delta$ 171.2, 169.6, 139.3, 128.6 (2 × CH), 122.9 (CH), 119.0 (2 × CH), 83.0 (C), 76.6 (CH), 69.4 (CH), 36.3 ($CH_2$), 32.1 ($CH_2$), 28.4 ($CH_2$), 28.3 ($CH_2$), 25.0 ($CH_2$), 24.8 ($CH_2$), 19.9 ($CH_3$). HRMS (ESI) $m/z$ [M + Na]$^+$ calcd for $C_{18}H_{24}O_3N_2Na$, 339.1679; found, 339.1682.

*O-Benzyl Suberoylanilide Hydroxamate (**2d**).* White solid (21.5 mg, 27% yield). $^1$H NMR (500 MHz, DMSO) $\delta$ 10.91 (s, 1H), 9.82 (s, 1H), 7.58 (d, $J$ = 7.6 Hz, 2H), 7.38 (d, $J$ = 4.4 Hz, 4H), 7.34 (m, 1H), 7.27 (m, 2H), 7.01 (t, $J$ = 7.4 Hz, 1H), 4.77 (s, 2H), 2.28 (t, $J$ = 7.4 Hz, 2H), 1.94 (t, $J$ = 7.3 Hz, 2H), 1.57 (m, 2H), 1.49 (m, 2H), 1.26 (m, 4H). $^{13}$C NMR (126 MHz, DMSO) $\delta$ 171.2, 169.3, 139.3, 136.1, 128.7, 128.6 (2 × CH), 128.2 (2 × CH), 128.2 (2 × CH), 122.9 (CH), 119.0 (2 × CH), 76.7 ($CH_2$), 36.3 ($CH_2$), 32.2 ($CH_2$), 28.4 ($CH_2$), 28.3 ($CH_2$), 25.0 ($CH_2$), 24.8 ($CH_2$). HRMS (ESI) $m/z$ [M + Na]$^+$ calculated for $C_{21}H_{26}O_3N_2Na$, 377.1835; found, 377.1836.

*O-(4-Propagyloxybenzyl) Suberoylanilide Hydroxamate (**2e**).* White solid (30 mg, 32% yield). $^1$H NMR (500 MHz, DMSO) $\delta$ 10.86 (s, 1H), 9.82 (s, 1H), 7.58 (d, $J$ = 7.7 Hz, 2H), 7.32 (d, $J$ = 8.6 Hz, 2H), 7.27 (m, 2H), 7.01 (t, $J$ = 7.4 Hz, 1H), 6.98 (d, $J$ = 8.6 Hz, 2H), 4.79 (d, $J$ = 2.4 Hz, 2H), 4.70 (s, 2H), 3.55 (t, $J$ = 2.4 Hz, 1H), 2.28 (t, $J$ = 7.4 Hz, 2H), 1.94 (t, $J$ = 7.3 Hz, 2H), 1.57 (m, 2H), 1.49 (m, 2H), 1.27 (m, 4H). $^{13}$C NMR (126 MHz, DMSO) $\delta$ 171.2, 169.3, 157.2, 139.3, 130.4 (2 × CH), 128.8, 128.6 (2 × CH), 122.9 (CH), 119.0 (2 × CH), 114.6 (2 × CH), 79.2, 78.2 (CH), 76.3 ($CH_2$), 55.4 ($CH_2$), 36.3 ($CH_2$), 32.2 ($CH_2$), 28.4 ($CH_2$), 28.3 ($CH_2$), 25.0 ($CH_2$), 24.8 ($CH_2$). HRMS (ESI) $m/z$ [M + Na]$^+$ calculated for $C_{24}H_{28}O_4N_2Na$, 431.1941; found, 431.1949.

## ASSOCIATED CONTENT

### Supporting Information

The Supporting Information is available free of charge on the ACS Publications website at DOI: 10.1021/acs.jmedchem.6b01426.

NMR spectra of derivatives **2a−e**, in vitro conversion analyses, biological methods (PDF)
Molecular formula strings (CSV)

## AUTHOR INFORMATION

### Corresponding Author

*Phone: 0044 1316518702. Fax: 0044 1317773520. E-mail: Asier.Unciti-Broceta@igmm.ed.ac.uk.

### Present Address

‡For J.T.W.: Centre for Innovative Cancer Therapeutics, Ottawa Hospital Research Institute, Ottawa, Ontario K1H 8L6, Canada.

### Author Contributions

All authors have given approval to the final version of the manuscript.

### Notes

The authors declare the following competing financial interest(s): The authors declare that a patent application (GB 1608716.5) is filed on compound **2e**.

## ACKNOWLEDGMENTS

We are grateful to the Alfonso Martín Escudero Foundation (B.R.-R.), the EC (H2020-MSCA-IF-2014-658833, Chemo-BOOM), and the EPSRC (EP/N021134/1) for financial support.



DOI: 10.1021/acs.jmedchem.6b01426
J. Med. Chem. XXXX, XXX, XXX−XXX

## ABBREVIATIONS USED

CuAAC, copper(I)-catalyzed alkyne−azide cycloaddition; DBU, 1,8-diazabicyclo(5.4.0)undec-7-ene; DMSO, dimethyl sulfoxide; $EC_{50}$, half-maximal effective concentration; HDAC, histone deacetylases; His, histidine; NSCLC, nonsmall-cell lung carcinoma; PBS, phosphate buffered saline; PEG, polyethylene glycol; ppm, parts per million; rt, room temperature; SAHA, suberoylanilide hydroxamic acid; SD, standard deviation; TLC, thin layer chromatography

## REFERENCES


(1) Versteegen, R. M.; Rossin, R.; ten Hoeve, W.; Janssen, H. M.; Robillard, M. S. Click to release: instantaneous doxorubicin elimination upon tetrazine ligation. *Angew. Chem., Int. Ed.* **2013**, *52*, 14112−14116.

(2) Murray, B. S.; Crot, S.; Siankevich, S.; Dyson, P. J. Potential of cycloaddition reactions to generate cytotoxic metal drugs in vitro. *Inorg. Chem.* **2014**, *53*, 9315−9321.

(3) Matikonda, S. S.; Orsi, D. L.; Staudacher, V.; Jenkins, I. A.; Fiedler, F.; Chen, J.; Gamble, A. B. Bioorthogonal prodrug activation driven by a strain-promoted 1,3-dipolar cycloaddition. *Chem. Sci.* **2015**, *6*, 1212−1218.

(4) Weiss, J. T.; Dawson, J. C.; Macleod, K. G.; Rybski, W.; Fraser, C.; Torres-Sánchez, C.; Patton, E. E.; Bradley, M.; Carragher, N. O.; Unciti-Broceta, A. Extracellular palladium-catalysed dealkylation of 5-fluoro-1-propargyl-uracil as a bioorthogonally activated prodrug approach. *Nat. Commun.* **2014**, *5*, 3277.

(5) Weiss, J. T.; Dawson, J. C.; Fraser, C.; Rybski, W.; Torres-Sánchez, C.; Bradley, M.; Patton, E. E.; Carragher, N. O.; Unciti-Broceta, A. Development and bioorthogonal activation of palladium-labile prodrugs of gemcitabine. *J. Med. Chem.* **2014**, *57*, 5395−5404.

(6) Weiss, J. T.; Fraser, C.; Rubio-Ruiz, B.; Myers, S. H.; Crispin, R.; Dawson, J. C.; Brunton, V. G.; Patton, E. E.; Carragher, N. O.; Unciti-Broceta, A. *N*-alkynyl derivatives of 5-fluorouracil: susceptibility to palladium-mediated dealkylation and toxigenicity in cancer cell culture. *Front. Chem.* **2014**, *2*, 56.

(7) Weiss, J. T.; Carragher, N. O.; Unciti-Broceta, A. Palladium-mediated dealkylation of *N*-propargyl-floxuridine as a bioorthogonal oxygen-independent prodrug strategy. *Sci. Rep.* **2015**, *5*, 9329.

(8) Sánchez, M. I.; Penas, C.; Vázquez, M. E.; Mascareñas, J. L. Metal-catalyzed uncaging of DNA-binding agents in living cells. *Chem. Sci.* **2014**, *5*, 1901−1907.

(9) Völker, T.; Dempwolff, F.; Graumann, P. L.; Meggers, E. Progress towards bioorthogonal catalysis with organometallic compounds. *Angew. Chem., Int. Ed.* **2014**, *53*, 10536−10540.

(10) Tonga, G. Y.; Jeong, Y.; Duncan, B.; Mizuhara, T.; Mout, R.; Das, R.; Kim, S. T.; Yeh, Y. C.; Yan, B.; Hou, S.; Rotello, V. M. Supramolecular regulation of bioorthogonal catalysis in cells using nanoparticle-embedded transition metal catalysts. *Nat. Chem.* **2015**, *7*, 597−603.

(11) Unciti-Broceta, A. Bioorthogonal catalysis: rise of the nanobots. *Nat. Chem.* **2015**, *7*, 538−539.

(12) Li, J.; Chen, P. R. Development and application of bond cleavage reactions in bioorthogonal chemistry. *Nat. Chem. Biol.* **2016**, *12*, 129−137.

(13) Yusop, R. M.; Unciti-Broceta, A.; Johansson, E. M. V.; Sánchez-Martín, R. M.; Bradley, M. Palladium-mediated intracellular chemistry. *Nat. Chem.* **2011**, *3*, 239−243.

(14) Unciti-Broceta, A.; Johansson, E. M. V.; Yusop, R. M.; Sánchez-Martín, R. M.; Bradley, M. Synthesis of polystyrene microspheres and functionalization with Pd(0) nanoparticles to perform bioorthogonal organometallic chemistry in living cells. *Nat. Protoc.* **2012**, *7*, 1207−1218.

(15) Li, J.; Yu, J.; Zhao, J.; Wang, J.; Zheng, S.; Lin, S.; Chen, L.; Yang, M.; Jia, S.; Zhang, X.; Chen, P. R. Palladium-triggered deprotection chemistry for protein activation in living cells. *Nat. Chem.* **2014**, *6*, 352−361.

(16) Codd, R. Traversing the coordination chemistry and chemical biology of hydroxamic acids. *Coord. Chem. Rev.* **2008**, *252*, 1387−1408.

(17) Grassadonia, A.; Cioffi, P.; Simiele, F.; Iezzi, L.; Zilli, M.; Natoli, C. Role of Hydroxamate-based histone deacetylase inhibitors (Hb-HDACIs) in the treatment of solid malignancies. *Cancers* **2013**, *5*, 919−942.

(18) Jomaa, H.; Wiesner, J.; Sanderbrand, S.; Altincicek, B.; Weidemeyer, C.; Hintz, M.; Türbachova, I.; Eberl, M.; Zeidler, J.; Lichtenthaler, H. K.; Soldati, D.; Beck, E. Inhibitors of the nonmevalonate pathway of isoprenoid biosynthesis as antimalarial drugs. *Science* **1999**, *285*, 1573−1576.

(19) Glozak, M. A.; Seto, E. Histone deacetylases and cancer. *Oncogene* **2007**, *26*, 5420−5432.

(20) Xu, W. S.; Parmigiani, R. B.; Marks, P. A. Histone deacetylase inhibitors: molecular mechanisms of action. *Oncogene* **2007**, *26*, 5541−5552.

(21) Grant, S.; Easley, C.; Kirkpatrick, P. Vorinostat. *Nat. Rev. Drug Discovery* **2007**, *6*, 21−22.

(22) Mann, B. S.; Johnson, J. R.; Cohen, M. H.; Justice, R.; Pazdur, R. FDA approval summary: vorinostat for treatment of advanced primary cutaneous T-cell lymphoma. *Oncologist* **2007**, *12*, 1247−1252.

(23) Marks, P. A. Discovery and development of SAHA as an anticancer agent. *Oncogene* **2007**, *26*, 1351−1356.

(24) Finnin, M. S.; Donigian, J. R.; Cohen, A.; Richon, V. M.; Rifkind, R. A.; Marks, P. A.; Breslow, R.; Pavletich, N. P. Structures of a histone deacetylase homologue bound to the TSA and SAHA inhibitors. *Nature* **1999**, *401*, 188−193.

(25) Chen, K.; Zhang, X.; Wu, Y. D.; Wiest, O. Inhibition and mechanism of HDAC8 revisited. *J. Am. Chem. Soc.* **2014**, *136*, 11636−11643.

(26) Santra, M.; Ko, S.-K.; Shin, I.; Ahn, K. H. Fluorescent detection of palladium species with an O-propargylated fluorescein. *Chem. Commun.* **2010**, *46*, 3964−3966.

(27) Tracey, M. P.; Pham, D.; Koide, K. Fluorometric imaging methods for palladium and platinum and the use of palladium for imaging biomolecules. *Chem. Soc. Rev.* **2015**, *44*, 4769−4791.

(28) Schmid, K. M.; Jensen, L.; Phillips, S. T. A self-immolative spacer that enables tunable controlled release of phenols under neutral conditions. *J. Org. Chem.* **2012**, *77*, 4363−4374.

(29) Major Jourden, J. L.; Daniel, K. B.; Cohen, S. Investigation of self-immolative linkers in the design of hydrogen peroxide activated metalloprotein inhibitors. *Chem. Commun.* **2011**, *47*, 7968−7970.

(30) Lang, K.; Chin, J. W. Bioorthogonal reactions for labeling proteins. *ACS Chem. Biol.* **2014**, *9*, 16−20.

(31) Singh, R. K.; Mandal, T.; Balasubramanian, N.; Cook, G.; Srivastava, D. K. Coumarin-suberoylanilide hydroxamic acid as a fluorescent probe for determining binding affinities and off-rates of histone deacetylase inhibitors. *Anal. Biochem.* **2011**, *408*, 309−315.

(32) Thomas, M.; Rivault, F.; Tranoy-Opalinski, I.; Roche, J.; Gesson, J. P.; Papot, S. Synthesis and biological evaluation of the suberoylanilide hydroxamic acid (SAHA) beta-glucuronide and beta-galactoside for application in selective prodrug chemotherapy. *Bioorg. Med. Chem. Lett.* **2007**, *17*, 983−986.

(33) Denis, I.; El Bahhaj, F.; Collette, F.; Delatouche, R.; Gueugnon, F.; Pouliquen, D.; Pichavant, L.; Héroguez, V.; Grégoire, M.; Bertrand, P.; Blanquart, C. Vorinostat-polymer conjugate nanoparticles for Acid-responsive delivery and passive tumor targeting. *Biomacromolecules* **2014**, *15*, 4534−4543.

(34) Daniel, K. B.; Sullivan, E. D.; Chen, Y.; Chan, J. C.; Jennings, P. A.; Fierke, C. A.; Cohen, S. M. Dual-mode HDAC prodrug for covalent modification and subsequent inhibitor release. *J. Med. Chem.* **2015**, *58*, 4812−4821.

(35) Alouane, A.; Labruère, R.; Le Saux, T.; Schmidt, F.; Jullien, L. Self-immolative spacers: kinetic aspects, structure-property relationships, and applications. *Angew. Chem., Int. Ed.* **2015**, *54*, 7492−7509.

(36) Binauld, S.; Damiron, D.; Hamaide, T.; Pascault, J.-P.; Fleury, E.; Drockenmuller, E. Click chemistry step growth polymerization of novel $\alpha$-azide-$\omega$-alkyne monomers. *Chem. Commun.* **2008**, *35*, 4138−4140.




DOI: 10.1021/acs.jmedchem.6b01426
J. Med. Chem. XXXX, XXX, XXX−XXX